Nano Energy 144 (2025) 111380

Contents lists available at ScienceDirect

Nano Energy

journal homepage: www.elsevier.com/locate/nanoen

Synergistic effects in triboelectric charge-driven redox reactions

Mohsin Shah [a,b,1], Shaoxin Li [a,b,1], Zhe Yang [a,b,1], Jiajin Liu [a,b], Puguang Peng [a,b], Han Qian [a,b], Zhong Lin Wang [a,c,d,*], Di Wei [a,e,*]

[a] Beijing Institute of Nanoenergy and Nanosystems, Chinese Academy of Sciences, Beijing 101400, PR China
[b] School of Nanoscience and Engineering, University of Chinese Academy of Sciences, Beijing 100049, PR China
[c] Beijing Key Laboratory of Micro-Nano Energy and Sensor, Center for High-Entropy Energy and Systems, Beijing Institute of Nanoenergy and Nanosystems, Chinese Academy of Sciences, Beijing 101400, PR China
[d] Guangzhou Institute of Blue Energy, Knowledge City, Huangpu District, Guangzhou 510555, PR China
[e] Centre for Photonic Devices and Sensors, University of Cambridge, 9 JJ Thomson Avenue, Cambridge CB3 0FA, UK

ARTICLE INFO

Keywords:
Contact-Electro-Chemistry (CE-Chemistry)
Solid–liquid contact electrification
Metal ion reduction
Synergistic effects

ABSTRACT

Beyond conventional electrochemical processes, triboelectric charge-driven reactions from dielectric solid-liquid contact electrification (CE) define a distinct realm within Contact-Electro-Chemistry (CE-Chemistry). While recent studies have explored CE-Chemistry in pollutant degradation and metal reduction, the mechanisms governing electron transfer and radical formation, etc. remain unclear. This work first demonstrates that the efficiency of CE-driven metal ion reduction is governed not only by the ease of electron extraction from the solvent but also by the electron-donating properties of the dielectric, as evidenced by experimental results and DFT calculations. Aerobic and anaerobic conditions show that superoxide radicals ($\cdot O_2^-$) significantly contribute to silver ion (Ag^+) reduction, indicating a synergistic mechanism involving electron transfer and radical mediation. Surface modifications and solvent types were also examined for their influence on CE-driven Ag^+ reduction. A synergistic relationship between Ag^+ reduction and methyl orange (MO) oxidative degradation was observed, revealing coupled redox processes during the reaction. Additionally, the role of triboelectric charge generated by solid-solid CE in driving redox reactions was explored in aqueous systems. These findings deepen the mechanistic understanding of CE-Chemistry, uncovering new avenues for leveraging synergistic catalytic processes and enabling advancements in catalysis with tunable reaction kinetics.

1. Introduction

Mechanochemistry employs mechanical energy to induce chemical transformations under solvent-free or low-solvent conditions, aligning with green chemistry principles by reducing environmental footprint [1,2]. Mechanical forces induce site-selective bond cleavage through shear-induced disorder [3], molecular polarization [4], and activation of solid reagents [5], enabling transformations unattainable by conventional methods. Liquid-assisted grinding extends the synthetic scope by activating poorly soluble precursors, including sulfates, oxides, and carbonates, for the direct construction of metal-organic materials [6,7]. Despite its broad utility, mechanochemistry remains constrained by the intrinsic heterogeneity of mechanical stimuli, including compression [8], shear [9], impact [10], and extension [11], which often limit reproducibility and reaction efficiency. More recently, piezoelectric materials have emerged as promising mediators of mechano-redox processes, converting mechanical stress into interfacial electric fields via charge polarization [12]. However, commonly employed piezoelectric ceramics, including barium titanate and lead zirconate titanate, suffer from poor mechanical robustness, environmental toxicity, and rapid charge carrier recombination upon stress relaxation, collectively limiting their scalability and catalytic efficiency [13,14]. Sonochemistry is a subbranch of mechanochemistry that employs high-frequency ultrasound to induce acoustic cavitation and mechanical vibrations in liquid media, facilitating chemical reactions through localized high temperatures, pressures, and shear forces [15]. Sonochemical methods often exhibit low reaction rates, poor selectivity, and limited control over reaction pathways, reducing their practical utility [16]. Additionally, electrochemical reduction typically requires externally applied voltage and relies on complex instrumentation and experimental setups,

* Corresponding authors at: Beijing Institute of Nanoenergy and Nanosystems, Chinese Academy of Sciences, Beijing 101400, PR China.
E-mail addresses: zlwang@binn.cas.cn (Z.L. Wang), weidi@binn.cas.cn (D. Wei).
[1] These authors contributed equally: Mohsin Shah, Shaoxin Li, Zhe Yang.

https://doi.org/10.1016/j.nanoen.2025.111380
Received 30 June 2025; Received in revised form 29 July 2025; Accepted 10 August 2025
Available online 12 August 2025

posing challenges for operational simplicity and scalability [17]. Contact-Electro-Chemistry (CE-Chemistry) has recently emerged as a novel approach that harnesses triboelectric charges generated at solid-liquid interfaces during cyclic contact-separation to drive interfacial electron and radical transfer, offering a promising route for the activation and enhancement of chemical transformations [18,19]. In particular, Contact-Electro-Catalysis (CEC) utilizes these triboelectric charges arising from solid-liquid contact electrification (CE) to induce catalytic reactions [18,20]. Distinct from conventional electrochemical processes reliant on externally applied electric fields, CEC capitalizes on internally generated electric fields at material interfaces, introducing a new paradigm for triboelectric charge-mediated catalysis. This CE-driven strategy has attracted growing interest for its capacity to initiate and sustain diverse chemical reactions under mild conditions.

Studies have demonstrated that electron transfer predominates at solid-liquid interfaces [19,21–25]. Wang et al. introduced an electron cloud potential-well model to explain this phenomenon, where the interaction of two materials under external mechanical force causes their electron clouds to overlap, thereby lowering the energy barrier and promoting electron transfer between atoms [26,27]. Such solid-liquid CE-driven electron transfer provides the fundamental basis for chemical reactions [28,29]. In 2022, Wang et al. introduced the CEC strategy, where electron transfer during CE generates reactive oxygen species (ROS) and facilitating pollutant degradation [18]. Li et al. applied CEC to effectively leach metals from wastes of lithium-ion batteries through ultrasonication-induced cavitation, followed by metal separation and catalyst recovery [30]. It was further demonstrated that CEC facilitates methane conversion under ambient conditions by utilizing the electrification of fluorinated ethylene propylene (FEP) particles with water under ultrasound, yielding methanol and formaldehyde [31]. Their study emphasizes that electron transfer is the primary mechanism driving the reduction process. Additionally, they highlight the crucial role of dielectric materials, demonstrating that those with higher electronegativity and electron-withdrawing capacity significantly enhance reduction efficiency compared to their lower-electronegativity counterparts. Li, J. et al. reported ammonia synthesis from nitrogen gas in water containing PTFE microparticles, driven by contact electrification and using water as the proton source [32]. CE-Chemistry, as explored by Wei et al., harnesses these free radicals to drive reactions in areas such as CE-Redox, CE-Polymerization, CE-Catalysis, and CE-Fluorescence [33]. CE-Chemistry is pervasive across various processes, with triboelectric charge generated from flow electrification in dielectric tubes capable of initiating chemical reactions, demonstrating potential for real-time catalysis and metal reduction in wastewater treatment [20,34]. It should be noted that H^+ generated during CE in aqueous systems likely adsorb onto the negatively charged dielectric surface, forming an electrical double layer (EDL), which inhibits interfacial electron transfer and hinders CE-driven reactions. In contrast, the non-aqueous solvent, for example, dimethyl sulfoxide (DMSO) has been widely utilized as an organic medium for chemical reactions [35]. It was also reported to effectively mitigate the EDL screening effect, accelerating phenol degradation by over 40 times and potentially enhancing reaction efficiency in CE-driven systems [36]. Su et al. demonstrated that FEP particles facilitate the reduction of precious metal ions via CEC in aqueous media, under both aerobic and anaerobic conditions [37].

This study aimed to capture the full complexity of the mechanistic intricacies underlying CE-Chemistry in metal ion reduction. To achieve this, we utilized polytetrafluoroethylene (PTFE) and glass balls, which are positioned at opposite ends of the triboelectric series, exhibiting distinct electronegativities and differing electron-accepting and donating properties. Both materials exhibit robust stability, showing no signs of degradation or absorption, and can be efficiently recovered post-experiment through washing. This study redefines the CE-Chemistry mechanism for metal ion reduction, demonstrating that its efficiency is governed by both the propensity for electron extraction from the solvent and the electron-donating properties of the dielectric material. Density functional theory (DFT) calculations substantiate this hypothesis, offering deeper insight into the dielectric's role in catalyzing CE-driven metal ion reduction. For the first time, solid-liquid CE-based metal ion reduction is revealed to follow a synergistic dual mechanism, wherein Ag^+ reduction proceeds via direct electron transfer from the dielectric surface and the generation of superoxide radicals ($\cdot O_2^-$), formed as oxygen captures electrons from the dielectric. This dual mechanism, integrating electron exchange and radical-driven pathways, fundamentally reshapes the role of CE in chemical reactions. Electron Paramagnetic Resonance (EPR) spectroscopy was employed to analyze radical production and electron transfer dynamics, while oxygen plasma etching of the glass surface enhanced solid-liquid CE efficiency by improving surface interaction with the solution. Solvent effects also played a crucial role, with DMSO significantly enhancing reduction performance. Beyond mechanistic insights, a synergistic interplay between MO degradation and Ag^+ reduction under solid-liquid CE conditions was identified, where the glass surface facilitates Ag^+ reduction to nanoparticles, and in situ-generated AgNPs promote MO degradation without additional reagents or catalysts. Furthermore, this study explores solid-solid CE's role in governing charge interactions in aqueous solvents, establishing a broader framework for interfacial charge dynamics with profound implications for next-generation catalytic systems and material synthesis. By redefining the fundamental principles of CE-Chemistry, this work highlights its pivotal role in driving chemical reactions and underscores its potential integration with conventional electrochemistry to revolutionize catalysis, offering a more versatile, sustainable, and cost-effective strategy for advancing chemical processes across diverse industrial applications.

2. Results

2.1. Reduction of silver ions (Ag^+) in CE-Chemistry using glass balls

The solid-liquid CE process and its catalytic role in CE-Chemistry have been demonstrated under various conditions, including ultrasonication [32,38], flow electrification [20], and ball milling [39]. Ultrasonication is known to induce sonochemical effects, particularly at high frequencies (400–500 kHz), where acoustic cavitation generates reactive radical species [40]. To suppress such effects, ultrasonication in this study was conducted at a low frequency of 40 kHz, a regime in which chemical contributions are negligible and physical effects are dominant in classical sonochemistry. In addition, a full set of parallel control experiments without dielectric solids was conducted to distinguish sonochemical effects from triboelectrically induced CE-Chemistry in this study. Ultrasonication will induces repetitive contact-separation cycles at the solid dielectric-water interface through cavitation bubble collapse [41]. To investigate the solid-liquid CE mechanism in metal ion (Ag^+) reduction, 4 mm diameter glass and PTFE balls, possessing distinct electron-withdrawing and donating properties, were selected. These were separately immersed in 20 mL of 1 mM $AgNO_3$ solution and subjected to ultrasonication for 2 h, with measurements recorded at 30-minutes intervals, as shown in Figure S1. This process promotes electron cloud overlap between interacting materials, reducing the energy barrier and enhancing electron transfer efficiency. Within minutes, the solution containing glass balls transitioned from transparent to a bluish-black color, suggesting the possible formation of silver nanoparticles (AgNPs). In contrast, the solution with PTFE balls remained transparent throughout the ultrasonication process, irrespective of its duration (Figure S2). Comprehensive characterization using Transmission Electron Microscopy (TEM), Scanning Electron Microscopy (SEM), and Energy Dispersive X-ray Spectroscopy (EDX) further confirmed the reduction of Ag^+ to AgNPs, as illustrated in Figure 1a–c, S3. Ultraviolet-Visible (UV-Vis) spectroscopy was conducted on samples comprising PTFE and glass balls individually. The glass-containing sample showed a significant increase in the 4d-5sp interband transition at 320 nm, with intensity rising over ultrasonication time, while no

surface plasmon resonance (SPR) absorption band was detected (Fig. 1d). According to the literature, when AgNPs form in solution, metallic silver exhibits a SPR absorption band in the visible range of 350–550 nm, while Ag 4d-5sp interband transitions typically occur around 320 nm [42–44]. The SPR absorption band of AgNPs is governed by factors such as size, shape, concentration, dielectric properties of both the nanoparticles and surrounding medium, and aggregation, with particles outside the 10–100 nm range typically failing to exhibit an SPR absorption band [45,46]. In our experiment, the absence of a chemical stabilizer may lead to AgNPs aggregation, yielding nanoparticles in the 300–500 nm size range, as confirmed by TEM analysis, significantly larger than the typical size range associated with an SPR absorption band (Figure S4). However, when the experiment was conducted with a lower concentration of 0.1 mM $AgNO_3$ solution, a distinct SPR absorption band appeared and increased in intensity with prolonged ultrasonication, indicating the formation of smaller nanoparticles at lower concentrations (Figure S5). Figure S6 demonstrates that, in contrast, the PTFE-containing sample exhibited neither a detectable Ag 4d–5sp interband transition nor an SPR absorption band. As illustrated in Fig. 1e, quantitative analysis via inductively coupled plasma optical emission spectroscopy (ICP-OES) confirmed that PTFE balls, compared to glass balls, exhibit an extremely low Ag^+ reduction capability of approximately 3–4 % under ambient conditions. Additionally, no discernible color change was observed in the solution, and TEM analysis (Figure S7) reveals that the AgNPs formed in the PTFE-containing sample are significantly smaller than those in the glass-containing sample. Collectively, these findings suggest that the minimal reduction performance of PTFE is responsible for the absence of both the SPR absorption band and Ag 4d–5sp interband transitions.

Previous studies that synthesized AgNPs via various chemical and biological methods have reported that $\cdot O_2^-$ can facilitate Ag^+ reduction (25, 26). To elucidate the mechanism underlying Ag^+ reduction, this study sought to determine whether the process was driven by $\cdot O_2^-$ or direct electron transfer from the dielectric. Here, singlet oxygen ($^1O_2$) was detected using 0.10 M 2,2,6,6-tetramethyl-4-piperidone (TEMP) during ultrasonication in DI water in the presence of PTFE and glass. It is generally believed that $^1O_2$ is a product of the oxidation of $\cdot O_2^-$ radicals, thereby confirming the presence of $\cdot O_2^-$ radicals [47]. Fig. 2a shows that the triplet peak corresponding to the TEMP-$^1O_2$ adduct in the glass sample has a slightly higher intensity than in the PTFE sample, likely contributing to the more pronounced reduction of Ag^+ in the glass sample with more $\cdot O_2^-$ radicals. In contrast, the almost invisible reduction of Ag^+ in the PTFE system is hypothesized due to its highly oxidative environment generated by ·OH. As shown in Fig. 2b, EPR analysis using 0.10 M 5,5-dimethyl-1-pyrroline N-oxide (DMPO) as a radical trapping agent revealed the characteristic quadruplet peaks of DMPO-·OH. The significantly more intense peaks observed in the PTFE system, compared to the glass system, confirm a higher yield of ·OH, indicating a more oxidative environment. These strong oxidative conditions likely suppress Ag^+ reduction, thereby inhibiting AgNPs formation. To gain further insights into the electron transfer dynamics, the reduction of 2,2,6,6-Tetramethylpiperidine 1-oxyl (TEMPO), a paramagnetic electron scavenger, during ultrasonication in DI water in the presence of PTFE and glass balls was also investigated using EPR spectroscopy [37]. The reduction of TEMPO to its non-paramagnetic form, TEMPOH, results in a decrease in the EPR signal intensity. Notably, a more substantial reduction of TEMPO was observed in the PTFE system compared to the glass system, suggesting that the PTFE surface acquires more electrons

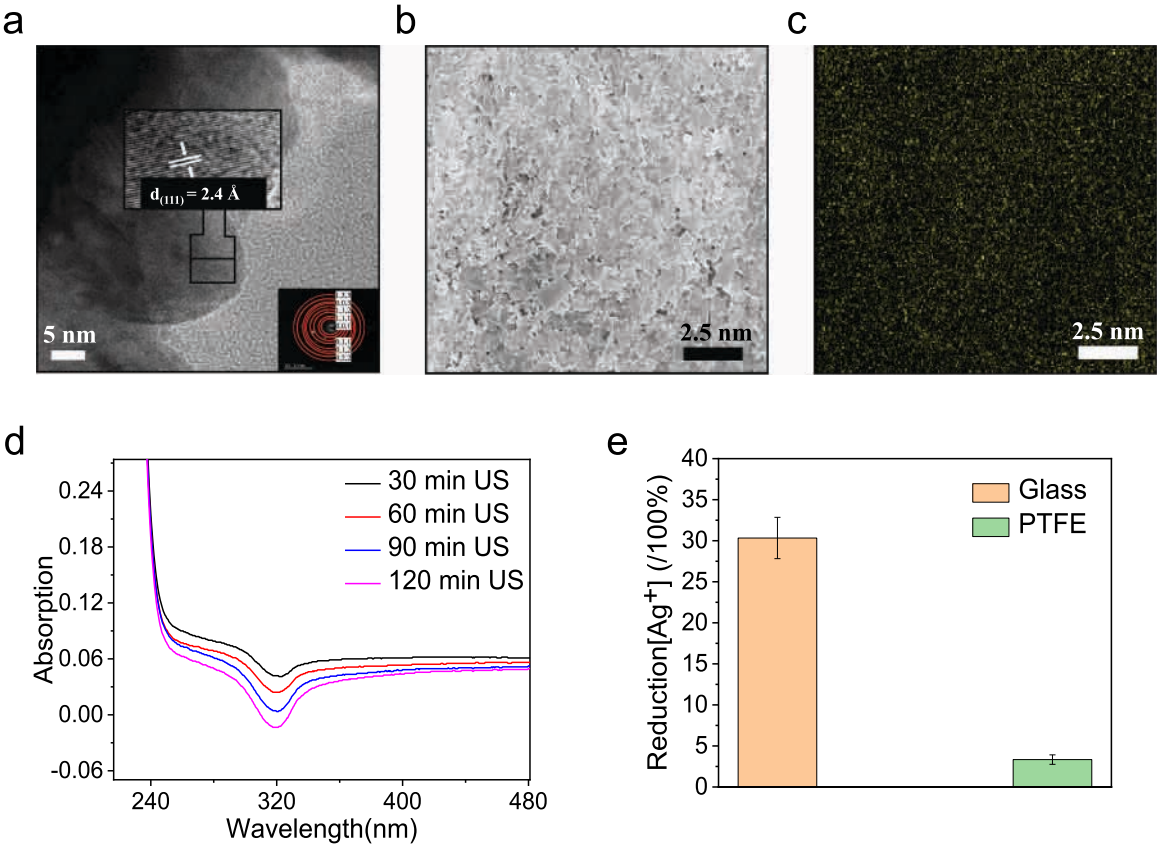

Fig. 1. Characterization of Ag^+ reduction to AgNPs. a) TEM photograph of AgNPs and measurement of d-spacing, insets contain the SAED pattern of the particles. b) SEM photograph of particle AgNPs. c) EDX mapping of AgNPs. d) UV-Vis absorption plot of $AgNO_3$ solution (concentration 1 mM) containing glass balls during 2-Hour US with 30-minutes intervals. e) The reduction of Ag^+ in aqueous solution mediated by glass/PTFE dielectrics via CE after 1 h. Error bars represent the standard deviations from three independent experiments.

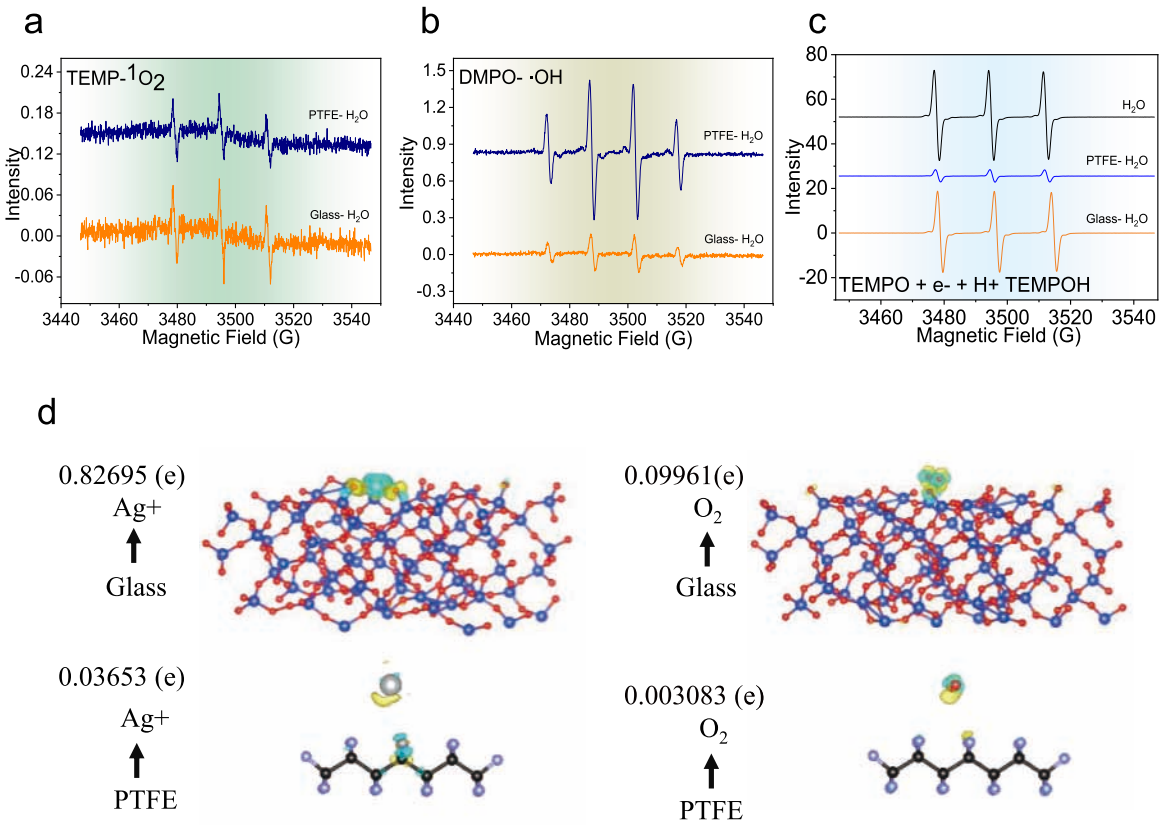

Fig. 2. Schematic radical generation and product formation in CE-Chemistry. a) EPR spectroscopic analysis of TEMP signals in PTFE and Glass. b) EPR Spectroscopic analysis of DMPO signals in PTFE and Glass. c) EPR Spectroscopic analysis of TEMPO signals in PTFE and Glass. d) Simulated spatial distribution of charge density difference between Ag^+/ O_2 molecules and PTFE/Glass surfaces, highlighting the charge transfer interactions.

during solid-liquid CE, as illustrated in Fig. 2c. This behavior can be attributed to the presence of highly electronegative fluorine atoms in PTFE, which attract electrons, making it more likely to acquire electrons in this process. As Ag^+ ions can be reduced upon receiving electrons from a negatively charged dielectric, the surface characteristics of the dielectric play a crucial role in determining its electron-donating properties. The enhanced Ag^+ reduction in the glass system was proposed to arise from oxygen-containing functional groups on the glass surface, which, due to their stronger electron-donating properties compared to fluorine in PTFE, facilitate more efficient electron transfer to Ag^+ and oxygen molecules (O_2). To evaluate the contribution of sonochemical effects in the absence of a dielectric interface, a control experiment was performed under identical ultrasonication conditions but without the dielectric material. As shown in Figure S8, no discernible reduction of Ag^+ was observed, indicating that ultrasonication alone does not induce the reduction process. The reduction of Ag^+ is believed to proceed via direct electron transfer from the dielectric surface, while electrons transferred to O_2 generate $\cdot O_2^-$, which synergistically enhances the process. Previous studies have demonstrated that charge transfer at solid-liquid interfaces can be effectively evaluated using density functional theory (DFT), offering important insights into the mechanisms of CE in aqueous systems [48]. Charge transfer is anticipated when a solid during solid-liquid CE, which is a fundamental characteristic of CE. To validate our hypothesis regarding the different electron-donating abilities of glass and PTFE surfaces, DFT calculations were performed to quantify the charge transfer from these materials to Ag^+ and O_2 during solid-liquid CE. The charge density difference reveals the spatial distribution of charge migration within each system, with yellow regions representing charge accumulation and blue regions indicating charge depletion, as shown in Fig. 2d. Quantitative Bader charge analysis indicates that the charge transfer from the glass surface to Ag^+ (0.82695 e) is significantly higher than that observed from PTFE to Ag^+ (0.03653 e), with a difference of approximately 22.6 times. This considerable disparity suggests that the glass surface exhibits a stronger electron-donating capability towards Ag^+. Similarly, the charge transfer from the glass surface to O_2 (0.09961 e) is markedly higher compared to the charge transfer observed from PTFE to O_2 (0.003083 e), with a difference of approximately 32.3 times The observed differences in charge transfer are attributed to the intrinsic chemical properties of the materials. The silicate network structure of glass, rich in oxygen atoms and exhibiting structural flexibility, facilitates the donation of electron density to both Ag^+ and O_2. In contrast, PTFE, characterized by highly electronegative fluorine atoms and stable C-F bonds, exhibits a significantly reduced electron-donating capacity. These results provide strong theoretical support for the hypothesis that the glass surface enhances electron transfer, where direct electron donation and $\cdot O_2^-$ generation synergistically facilitate Ag^+ reduction.

To further elucidate the relationship between reduction efficiency and surface characteristics, the glass substrate was subjected to oxygen plasma etching. This treatment is expected to facilitate the incorporation of oxygenated surface functional groups, such as hydroxyl (-OH) and carboxyl (-COOH) moieties etc., thereby enhancing surface polarity [49, 50]. As shown in Figure S9, the reduction efficiency of Ag^+ was slightly increased following surface modification. The modest improvement in reduction activity is believed to result from the enhancement in surface properties induced by plasma treatment. Oxygen plasma treatment removes organic contaminants, dust, and other impurities, improving the surface's interaction with materials. This is also believed to cause a slight increase in surface hydrophilicity through the incorporation of oxygen-containing functional groups, contributing to the observed effect. To evaluate this, we measured the contact angle of water on the glass surface before and after plasma etching. Figure S10 shows a slight

reduction in contact angle was observed, indicating modest enhancement in hydrophilicity and a corresponding improvement in reduction efficiency. These results suggest that surface modification also plays a role in the mechanism of CE-Chemistry.

2.2. Proposed mechanism of Ag^+ reduction in CE-Chemistry

To investigate the role of $\cdot O_2^-$, which typically arises from the reduction of oxygen, experiments were conducted under different atmosphere conditions, including argon (anaerobic), oxygen (aerobic), and ambient air. As shown in Figure S11-S12, the reduction of Ag^+ in the glass system was significantly enhanced under anaerobic conditions compared to that observed under ambient environment. It is proposed that, in the absence of oxygen, electrons captured by the glass surface are efficiently transferred to Ag^+ from the dielectric surface, thereby facilitating Ag^+ reduction. This is supported by our DFT results, which also eliminate the possibility that only $\cdot O_2^-$ radicals are responsible for Ag^+ reduction. Besides, under aerobic conditions, the reduction of Ag^+ in the glass system was also markedly enhanced relative to that under ambient atmosphere (Figure S13-S14). Such enhancement is likely attributed to the increased availability of oxygen, which facilitates the generation of more $\cdot O_2^-$ to promote Ag^+ reduction A control experiment was conducted by introducing O_2 under otherwise identical ultrasonication conditions, but in the absence of the glass dielectric material, to rule out any contribution from sonochemistry in promoting Ag^+ reduction under aerobic conditions. As shown in Figure S15, no noticeable reduction of Ag^+ was observed, confirming that the enhanced Ag^+ reduction is not driven by sonochemical effects. In contrast, the PTFE system consistently exhibited minimal Ag^+ reduction across anaerobic, aerobic, and ambient atmosphere conditions, as shown in Figure S11-S14. This might because the characteristic of PTFE system generates higher levels of ·OH in solid-liquid CE, which creates a highly oxidative environment. In summary, within the glass system, electron transfer from water to the glass surface due to the solid-liquid CE effect, occurs through two primary pathways: some of the transferred electrons directly reduce Ag^+ ions at the glass surface, some of electrons are transferred to oxygen, generating $\cdot O_2^-$ radicals that further promote Ag^+ reduction (Fig. 3).

2.3. Non-aqueous CE-Chemistry

In aqueous systems, CE-Chemistry has been systematically studied, revealing a strong tendency to form an EDL screening effect that inhibits interfacial electron transfer. This phenomenon arises from the adsorption of H^+ ions onto the negatively charged dielectric surface, impeding the dynamics of CE-Chemistry reactions. On the other hand, the generation of ·OH radicals in aqueous systems is generally unfavorable for reduction reactions. To broaden the applicability of CE-Chemistry in reduction, the process was systematically investigated in an organic system using DMSO as a solvent. Moreover, DMSO offers relatively low toxicity compared to many other organic solvents, making it a more environmentally benign choice for non-aqueous CE-Chemistry. In this system, dimethyl sulfoxide (DMSO) acts as an electron donor upon contact with dielectric, resulting in the formation of methyl radicals ($\cdot CH_3$) and other reactive intermediates (DMSO*), while dielectric becomes negatively charged [36]. Notably, both PTFE and glass exhibited significantly enhanced catalytic activity in DMSO compared to DI water, as shown in Figure S16. This pronounced improvement in reduction efficiency highlights the crucial role of solvent properties in governing electron transfer dynamics. The enhanced catalytic activity in DMSO is likely due to its low ion concentration [36], which minimizes the EDL screening effect and facilitates more efficient electron transfer between the dielectric surface and reactants. Additionally, molecular oxygen exhibits significantly greater solubility in DMSO than in water, resulting in increased local oxygen availability near the reactive interface [51]. This elevated oxygen concentration enhances its ability to accept electrons from the dielectric surface, subsequently promoting the reduction of Ag^+ ions. Moreover, DMSO itself exhibits intrinsic reducing capabilities and has been reported to directly reduce molecular oxygen to $\cdot O_2^-$ even in the absence of external electron donors [52]. The generation of such reactive oxygen species further amplifies the overall reduction efficiency. This enhanced electron transfer mechanism consequently accelerates the reduction process. Notably, under ambient conditions, glass exhibits higher reduction efficiency than PTFE in DMSO, aligning with its stronger electron-donating ability observed in DI water. As demonstrated previously, no ·OH radicals were detected in DMSO, consistent with previous findings where DMSO acted as a scavenger for ·OH [36]. I In such an environment, $\cdot O_2^-$ is likely to play a pivotal role in the reduction mechanism. In the PTFE system, a contrast is observed

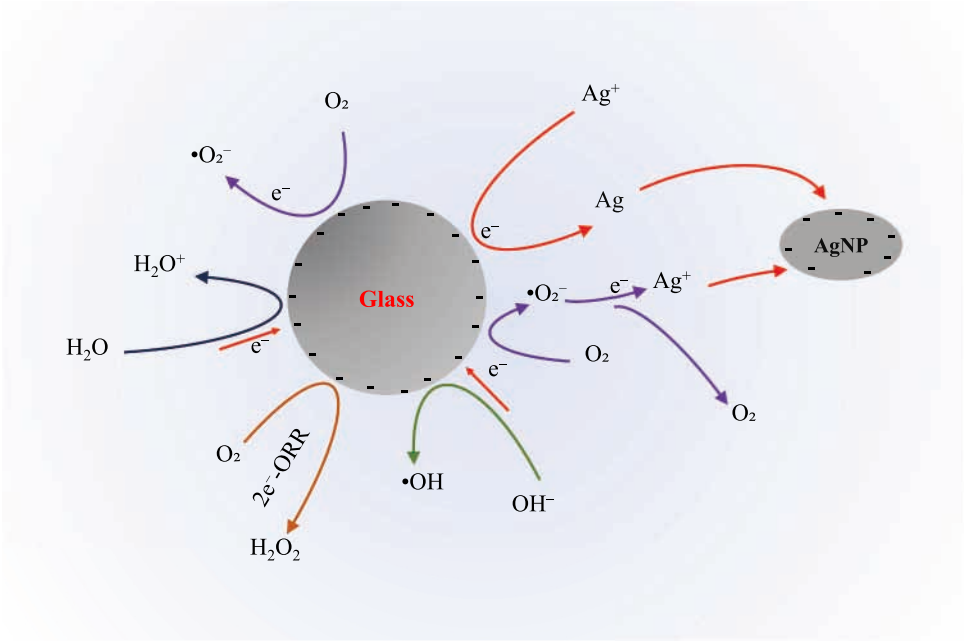

Fig. 3. Schematic of the mechanistic pathway showing electron acquisition by glass, superoxide radical generation via solid-liquid CE, and Ag^+ reduction to AgNPs.

with aqueous systems under ambient conditions, where the environment is more oxidative due to the higher presence of ·OH, inhibiting the involvement of $\cdot O_2^-$ in the reduction process. In DMSO, the enhanced electron transfer and increased generation of $\cdot O_2^-$ work synergistically to promote the reduction process, resulting in enhanced Ag^+ reduction in both the PTFE and glass systems. The experiment was also repeated in both aerobic and anaerobic systems, revealing significantly improved reduction performance for both PTFE and glass, further aligning with the mechanism verified in aqueous systems (Figure S17). X-ray photoelectron spectroscopy (XPS) was further employed to analyze the surface chemical composition of glass and PTFE dielectric balls before and after the reaction. The analysis, conducted after ultrasonication for 2 h in DI water and DMSO, revealed no significant changes in the surface composition (Figure S18). These findings indicate that glass and PTFE dielectrics exhibit high chemical and mechanical stability, contributing to their excellent recyclability.

2.4. Synergetic effect of and Ag^+ reduction and MO degradation

The degradation of the azo dye MO has been the subject of extensive research over the past few decades, with various strategies being explored to enhance its degradation efficiency [53–56]. Among these strategies, the use of nanoparticles, particularly AgNPs, has emerged as a promising approach due to their unique catalytic properties [57–59]. AgNPs are synthesized through methods such as chemical reduction, physical techniques, biological processes, green synthesis methods, and electrochemical methods, offering versatile preparation options. Various studies have synthesized AgNPs using these methods and subsequently employed photocatalysis to utilize the synthesized AgNPs for the degradation of pollutant dyes, such as MO [60]. Recently, numerous studies have also successfully employed CEC for the degradation of MO [18,61]. Given the growing interest in CEC-mediated MO degradation, the catalytic performance of glass was evaluated. Glass balls, identical in number and diameter to those used in the reduction experiments, were employed. However, no significant MO degradation was observed within two hours of ultrasonication (Figure S19). This outcome is ascribed to the crucial role of reactive ROS, particularly ·OH, as key drivers of MO degradation. As previously discussed, the reduced ·OH generation capacity of glass likely accounts for its poor catalytic efficiency in this process. However, upon introducing $AgNO_3$ into the aqueous system, a pronounced enhancement in MO degradation by the glass balls was observed (Fig. 4a). Given the prior findings demonstrating the ability of glass to facilitate the reduction of Ag^+ ions to nanoparticles, this enhancement is ascribed to the catalytic role of in-situ generated AgNPs. Prolonged ultrasonication facilitated continuous nanoparticle formation, progressively enhancing MO degradation efficiency. This was evidenced by the fading of MO's color, a decline in its UV–vis absorption peak, and an increase in silver inter-band transitions around 320 nm (Figure 4b and S19).

The underlying mechanism is proposed to involve AgNPs enhancing the generation of reactive ROS, thereby accelerating MO degradation [58,62]. The production of H_2O_2 in CEC systems is well-documented, with recent studies confirming the effective generation of H_2O_2 through CEC [38,63]. In this process, H_2O_2 is proposed to form via CEC involving AgNPs and glass through the two-electron oxygen reduction reaction ($2e^-$ ORR) and a less favorable two-electron water oxidation reaction ($2e^-$ WOR) pathway [64,65]. Furthermore, interactions between H_2O_2 and AgNPs have been reported to induce the formation of ·OH, as well as the generation of $\cdot O_2^-$ by AgNPs through the transfer of surface electrons to dissolved oxygen, along with their corresponding reaction kinetics [65–68]. It has also been reported that hydroxide ions (OH^-) can lose an electron to AgNPs to generate ·OH [58]. In the present study, it is proposed that both H_2O_2 and OH^- interact with AgNPs to produce ·OH radicals. Simultaneously, the surface of AgNPs acts as an electron reservoir, facilitating electron transfer to molecular oxygen and promoting the formation of $\cdot O_2^-$[62,68]. It is well-established that surface-trapped electrons on AgNPs play a crucial role in redox processes by reducing molecular oxygen to $\cdot O_2^-$, without altering the metallic Ag^0 core [68]. In contrast, the direct oxidation of AgNPs by oxygen is kinetically unfavorable. Moreover, $\cdot O_2^-$ can donate electrons back to the AgNPs surface, reinforcing a dynamic and reversible redox cycle at the nanoparticle interface [62]. This continuous electron exchange sustains the generation of reactive oxygen species, including $\cdot O_2^-$ and hydroxyl radicals (·OH), the latter formed primarily through the reaction of H_2O_2 with the AgNP surface. The combined action of ·OH and $\cdot O_2^-$ radicals play a crucial role in the enhanced degradation of MO. Fig. 4c presents a schematic representation of the synergistic process of AgNPs synthesis and MO degradation. Based on the observed results, the following reaction mechanism is proposed to explain the production of reactive radicals.

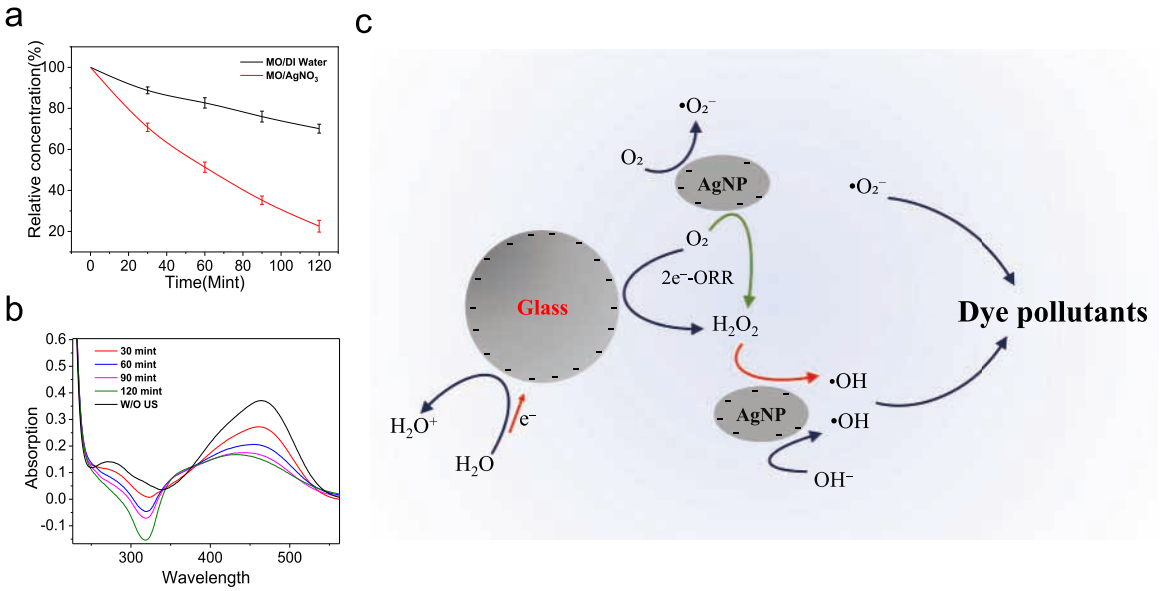

Fig. 4. Ag^+ reduction and MO degradation, mechanistic insight. a) MO degradation performance of Glass with and without $AgNO_3$, Error bars represent the standard deviations from three independent experiments. b) UV-Vis spectra of MO-$AgNO_3$ solution during 2-Hour ultrasonication with Glass Balls. c) Schematic of the mechanistic pathway for synergistic AgNPs synthesis and MO degradation.

$$O_2 + 2H^+ + 2e^- \rightarrow H_2O_2 \text{ (2e}^- \text{ ORR)} \quad (1)$$

$$2H_2O \rightarrow H_2O_2 + 2H^+ + 2e^- \text{ (2e}^- \text{ WOR)} \quad (2)$$

$$\cdot O_2^- + \cdot O_2^- + 2H^+ \rightarrow 2H_2O_2 + O_2 \quad (3)$$

$$AgNPs^{*-} + O_2 \rightarrow AgNPs + \cdot O_2^- \quad (4)$$

$$AgNPs + H_2O_2 \rightarrow Ag^+ + \cdot OH + OH^- \quad (5)$$

The synergistic approach to dye degradation via CE-Chemistry offers a compelling alternative to traditional electrochemical and photocatalytic methods. Conventional systems require external energy inputs, such as applied voltage or light irradiation, as well as complex setups and additional reagents, all of which contribute to higher operational costs and environmental burdens. Moreover, existing methods depend on AgNPs synthesized through multi-step processes that involve additional reagents. In contrast, the CE-driven process enables the in-situ generation of AgNPs, eliminating the need for external nanoparticle synthesis and reducing reagent consumption, process complexity, and environmental impact. This approach of synergistic in-situ AgNPs formation and dye degradation enhances efficiency, cost-effectiveness, and environmental sustainability, offering a more practical and viable alternative to conventional organic pollutant degradation strategies.

2.5. Influence of solid-solid contact electrification in CE-Chemistry

Triboelectrification, the process by which two materials acquire opposite charges upon contact and subsequent separation, has long been recognized for its role in chemical reactions [69]. The ability of triboelectrically charged dielectrics to facilitate redox processes has been demonstrated in several studies. Bard et al. use electrochemical experiments to demonstrate various chemical reactions triggered by pre-charged PTFE, including pH increase, hydrogen formation, metal deposition, and reduction of $Fe(CN)_6^{3-}$ [70]. Wang et al. demonstrated that CE between oppositely charged microdroplets generates exceptionally strong electric fields, reaching ~10^9 V/m. These fields have been shown to dissociate water molecules, producing ·OH, which play a crucial role in CEC[71]. Recent studies have primarily focused on continuous CE processes, such as ultrasound or ball milling of dielectrics in solution, rather than on the approach of pre-charging dielectric materials and subsequently immersing them in solution to initiate redox reactions [72–74]. This study investigates the influence of solid-solid contact electrification between two dielectrics, each exhibiting different surface charge densities after contact with water and immersion in solution, on CE-chemistry, as illustrated in Supplementary Figure S20. Unlike previous methods that rely on pre-charged dielectrics, this approach focuses on dynamic solid-liquid CE within the reaction medium. This paper examines whether continuous CE cycles at solid-solid interfaces within aqueous and non-aqueous media can generate localized electric fields that modulate redox reactions. An experimental setup was designed in which an equal number of PTFE and glass balls, each with a diameter of 4 mm (30 balls of each material), were employed. These materials, with opposing triboelectric properties and initially uncharged, were immersed in a 20 mL solution of 1 mM potassium ferrocyanide to investigate their influence on interfacial electron transfer processes. The system was subjected to ultrasonication for 2 h, with sampling intervals of 30 min. To verify whether repetitive CE cycles between the dielectric materials generate an electric field that breaks water molecules into ·OH, promoting redox reactions and driving the oxidation of ferrocyanide to ferricyanide, experiments were conducted with both PTFE-glass and PTFE-only systems. The results were compared to a control sample containing only PTFE balls, for which highly efficient solid-liquid CE oxidative performance has been previously reported in the literature [18,33,75]. The oxidation of ferrocyanide to ferricyanide was found to be marginally more efficient in the system containing only PTFE balls, demonstrating a slight enhancement in catalytic activity compared to the mixed PTFE-glass system (Fig. 5a). To further confirm these results, the experiment was repeated using nylon balls, which are also triboelectrically positive, yielding similar outcomes. PTFE exhibited the highest performance, followed by the PTFE-nylon mixed system, and lastly the nylon-only system (Figure S21).

To elucidate the reduced catalytic performance observed in the PTFE-glass system, electron EPR spectroscopy was employed to probe the electron dynamics and radical species implicated in the oxidation process. Fig. 5b showed a more substantial reduction of TEMPO was recorded in the PTFE system compared to both the PTFE-glass and glass-only systems, suggesting that the PTFE surface exhibits a higher propensity for electron acquisition. Furthermore, the utilization of DMPO, a ·OH scavenger, revealed a pronounced EPR signal in the PTFE system, indicative of enhanced ·OH production relative to both the mixed PTFE-glass and glass-only systems, as shown in Fig. 5c. To further confirm this, we conducted a terephthalic acid (THA) fluorescence assay, wherein THA was employed as a scavenger for ·OH, enabling the monitoring of their generation through an increase in fluorescence intensity corresponding to the THA-OH adduct [30,76]. The fluorescence data revealed a significant enhancement in signal intensity in the PTFE system, followed by the PTFE-glass system, and the glass-only system, corroborating the higher production of ·OH in the PTFE system (Fig. 5d). Taken together, these findings suggest that PTFE plays a predominant role in driving the oxidation process. In the PTFE-glass composite system, it is proposed that the electric field generated from solid-solid CE is insufficient to break water molecules into oxidative radicals. Furthermore, the presence of glass balls slightly impedes the solid-liquid interaction between PTFE and the solution, leading to a marginal decrease in CE-Chemistry efficiency and, consequently, a slight reduction in catalytic performance We also examined the effect of varying the PTFE-to-glass ball ratio while keeping the total number of balls constant (1:3). The results corroborate our findings that increasing the proportion of glass balls leads to reduced reaction efficiency. This suggests that glass impedes the solid–liquid interactions between PTFE and the solution, rather than enhancing the process through solid–solid contact electrification. The experiment was also repeated for MO degradation, and consistent with our observations, the PTFE-only system exhibited higher degradation efficiency than the combined PTFE–glass system (Figure S23). This indicates that in this mixed system, the overall CE-Chemistry reaction efficiency is primarily determined by the solid-liquid pair with the greatest electronegativity difference, as the area and probability of solid-liquid contact are much greater than those of solid-solid contact in the system.

3. Conclusion

In conclusion, this study offers comprehensive insights into the mechanistic pathways governing solid-liquid CE-Chemistry, particularly in the context of Ag^+ reduction. It redefines the CE-Chemistry mechanism by demonstrating that reduction efficiency is governed by both the electron-extracting properties of the solvent and the electron-donating nature of the dielectric material. DFT calculations substantiate this, revealing the critical role of the dielectric in catalyzing CE-driven metal ion reduction. The glass system notably enhances Ag^+ reduction, while PTFE shows limited activity, underscoring the importance of surface chemistry in electron transfer processes. The study further identifies a dual mechanism for solid-liquid CE-based Ag^+ reduction, involving direct electron transfer from the dielectric and the generated of $\cdot O_2^-$ during CE. Solvent properties, particularly DMSO, significantly enhance reduction performance, with improvements observed under both aerobic and anaerobic conditions. The investigation also reveals a synergistic interaction between MO degradation and Ag^+ reduction under solid-liquid CE conditions, where the glass surface facilitates Ag^+ reduction and in situ-generated AgNPs drive MO degradation without the need for additional reagents or catalysts. The generation of ROS, particularly ·OH

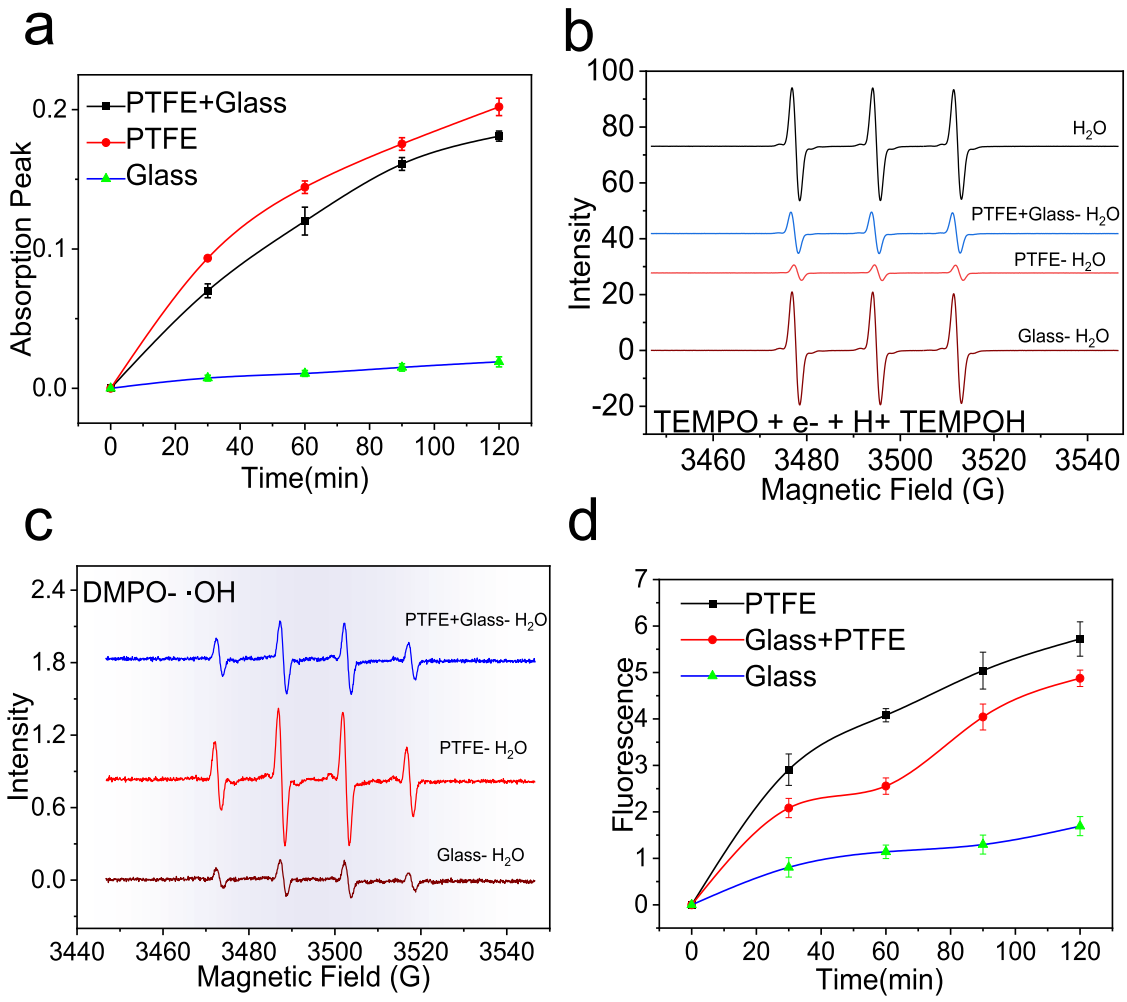

Fig. 5. Study on the S-S CE in CE-Chemistry. a) Increase in UV-Vis absorption peak of potassium ferrocyanide over time for PTFE-Glass, PTFE, and Glass systems, Error bars represent the standard deviations from three independent experiments. b) EPR spectroscopic analysis of TEMPO signals in PTFE-Glass, PTFE, and Glass Systems. c) EPR spectroscopic analysis of DMPO signals in PTFE-Glass, PTFE, and Glass Systems. d) Evaluation of ·OH radical production and reactivity in aqueous systems via THA-OH fluorescence and formazan dye absorbance.

radicals, plays a pivotal role in this catalytic process, with the synergistic effects of solid-liquid CE accelerating degradation, and AgNPs acting as efficient catalysts. The role of solid-solid CE in governing charge interactions is explored, showing that CE-Chemistry efficiency is primarily determined by the solid-liquid pair with the greatest electronegativity difference, due to the larger area and higher probability of solid-liquid contact. These findings provide new mechanistic insights into CE-driven metal ion reduction and open avenues for further exploration in pollutant dye degradation, precious metal reductions, and material optimization. This innovative paradigm provides fresh insights into the role of triboelectric charge in chemical transformations, paving the way for a deeper understanding of charge dynamics and their potential applications in catalysis and material synthesis.

CRediT authorship contribution statement

Mohsin Shah: Writing – review & editing, Writing – original draft, Visualization, Validation, Formal analysis. **Di Wei:** Writing – review & editing, Visualization, Validation, Supervision, Methodology, Funding acquisition, Formal analysis, Conceptualization. **Zhong Lin Wang:** Validation, Supervision, Conceptualization. **Han Qian:** Visualization, Methodology. **Puguang Peng:** Visualization, Software, Methodology. **Jiajin Liu:** Visualization, Software. **Zhe Yang:** Software. **Shaoxin Li:** Writing – review & editing, Formal analysis, Conceptualization.

Declaration of Competing Interest

The authors declare that they have no known competing financial interests or personal relationships that could have appeared to influence the work reported in this paper.

Acknowledgments

This work is financially supported by the National Natural Science Foundation (grant number 22479016).

Author contributions

D. Wei and Z.L. Wang designed research; M. Shah and S. Li performed research; Z. Yang performed DFT calculation; J. Liu performed ICP-OES; P. Peng performed SEM; H. Qian Performed EPR spectroscopy, and M. Shah, S. Li and D. Wei wrote the paper.

Data, materials, and software availability

All study data are included in the article, the supporting information.

Appendix A. Supporting information

Supplementary data associated with this article can be found in the online version at doi:10.1016/j.nanoen.2025.111380.

Data availability

Data will be made available on request.

References

[1] F. Cuccu, L.L. De, F. Delogu, E. Colacino, N. Solin, R. Mocci, A. Porcheddu, Mechanochemistry: new tools to navigate the uncharted territory of "impossible" reactions, ChemSusChem 15 (2022) e202200362, https://doi.org/10.1002/cssc.202200362.

[2] J.-L. Do, T. Friscic, Mechanochemistry: a force of synthesis, ACS Cent. Sci. 3 (2017) 13–19, https://doi.org/10.1021/acscentsci.6b00277.

[3] Y.S. Zholdassov, L. Yuan, S.R. Garcia, R.W. Kwok, A. Boscoboinik, D.J. Valles, M. Marianski, A. Martini, R.W. Carpick, A.B. Braunschweig, Acceleration of Diels-Alder reactions by mechanical distortion, Science 380 (2023) 1053–1058, https://doi.org/10.1126/science.adf5273.

[4] C. Wang, R. Zhao, W. Fan, L. Li, H. Feng, Z. Li, C. Yan, X. Shao, K. Matyjaszewski, Z. Wang, Tribochemically controlled atom transfer radical polymerization enabled by contact electrification, Angew. Chem. (Int. Ed. Engl.) 62 (2023) e202309440, https://doi.org/10.1002/anie.202309440.

[5] H.T. Baytekin, B. Baytekin, S. Huda, Z. Yavuz, B.A. Grzybowski, Mechanochemical activation and patterning of an adhesive surface toward nanoparticle deposition, J. Am. Chem. Soc. 137 (2015) 1726–1729, https://doi.org/10.1021/ja507983x.

[6] C.J. Adams, M.A. Kurawa, M. Lusi, A.G. Orpen, Solid state synthesis of coordination compounds from basic metal salts, CrystEngComm 10 (2008), https://doi.org/10.1039/b809950b.

[7] T. Friščić, L. Fábián, Mechanochemical conversion of a metal oxide into coordination polymers and porous frameworks using liquid-assisted grinding (LAG), CrystEngComm 11 (2009), https://doi.org/10.1039/b822934c.

[8] Y. Chen, G. Mellot, L.D. van, C. Creton, R.P. Sijbesma, Mechanochemical tools for polymer materials, Chem. Soc. Rev. 50 (2021) 4100–4140, https://doi.org/10.1039/d0cs00940g.

[9] F.H. Bhuiyan, Y.-S. Li, S.H. Kim, A. Martini, Shear-activation of mechanochemical reactions through molecular deformation, Sci. Rep. 14 (2024) 2992, https://doi.org/10.1038/s41598-024-53254-2.

[10] S.A. Humphry-Baker, S. Garroni, F. Delogu, C.A. Schuh, Melt-driven mechanochemical phase transformations in moderately exothermic powder mixtures, Nat. Mater. 15 (2016) 1280–1286, https://doi.org/10.1038/nmat4732.

[11] D. Wu, J.M. Lenhardt, A.L. Black, B.B. Akhremitchev, S.L. Craig, Molecular stress relief through a force-induced irreversible extension in polymer contour length, J. Am. Chem. Soc. 132 (2010) 15936–15938, https://doi.org/10.1021/ja108429h.

[12] Y. Feng, L. Ling, Y. Wang, Z. Xu, F. Cao, H. Li, Z. Bian, Engineering spherical lead zirconate titanate to explore the essence of piezo-catalysis, Nano Energy 40 (2017) 481–486, https://doi.org/10.1016/j.nanoen.2017.08.058.

[13] T.Y. Zhang, C.F. Gao, Fracture behaviors of piezoelectric materials, Theor. Appl. Fract. Mech. 41 (2004) 339–379, https://doi.org/10.1016/j.tafmec.2003.11.019.

[14] S.S. Anandakrishnan, M. Tabeshfar, M. Nelo, J. Peräntie, H. Jantunen, J. Juuti, Y. Bai, Recycling hazardous and energy-demanding piezoelectric ceramics using an oxide–halide perovskite upside-down composite method, RSC Sustain. 2 (2024) 961–974, https://doi.org/10.1039/d3su00348e.

[15] K.S. Suslick, Mechanochemistry and sonochemistry: concluding remarks, Faraday Discuss. 170 (2014) 411–422, https://doi.org/10.1039/c4fd00148f.

[16] P.A. Rosales, E.K. Esquivel, The evolution of sonochemistry: from the beginnings to novel applications, ChemPlusChem 89 (2024) e202300660, https://doi.org/10.1002/cplu.202300660.

[17] R.D. Little, K.D. Moeller, Introduction: electrochemistry: technology, synthesis, energy, and materials, Chem. Rev. 118 (2018) 4483–4484, https://doi.org/10.1021/acs.chemrev.8b00197.

[18] Z. Wang, A. Berbille, Y. Feng, S. Li, L. Zhu, W. Tang, Z.L. Wang, Contact-electro-catalysis for the degradation of organic pollutants using pristine dielectric powders, Nat. Commun. 13 (2022) 130, https://doi.org/10.1038/s41467-021-27789-1.

[19] Z. Wang, X. Dong, W. Tang, Z.L. Wang, Contact-electro-catalysis (CEC), Chem. Soc. Rev. 53 (2024) 4349–4373, https://doi.org/10.1039/d3cs00736g.

[20] C. Xu, S. Li, Y. Zhang, Z. Wang, Z.L. Wang, D. Wei, Contact-electro-chemistry induced by flow electrification in dielectric tubes, Nano Energy 134 (2025), https://doi.org/10.1016/j.nanoen.2024.110526.

[21] S. Lin, X. Chen, Z.L. Wang, Contact electrification at the Liquid-Solid interface, Chem. Rev. 122 (2022) 5209–5232, https://doi.org/10.1021/acs.chemrev.1c00176.

[22] T. Liu, X. Cui, Z. Ye, X. Li, Y. Liu, B. Luo, S. Zhang, M. Chi, J. Wang, C. Cai, Y. Bai, S. Wang, S. Nie, A pulsed Bubble-Driven efficient Liquid-Solid triboelectric nanogenerator, Adv. Funct. Mater. 35 (2024), https://doi.org/10.1002/adfm.202415483.

[23] B. Luo, X. Wang, T. Liu, C. Cai, Y. Liu, S. Zhang, M. Chi, C. Gao, J. Wang, Z. Liu, S. Wang, S. Nie, Liquid–Solid triboelectric probes for bubbles status monitoring, Adv. Funct. Mater. 34 (2024), https://doi.org/10.1002/adfm.202315725.

[24] B. Luo, T. Liu, C. Cai, J. Yuan, Y. Liu, C. Gao, X. Meng, J. Wang, S. Zhang, M. Chi, Y. Qin, J. Zhao, X. Zhuang, S. Wang, S. Nie, Triboelectric charge-separable probes for quantificationally charge investigating at the liquid-solid interface, Nano Energy 113 (2023), https://doi.org/10.1016/j.nanoen.2023.108532.

[25] B. Luo, C. Cai, T. Liu, S. Zhang, C. Gao, Y. Liu, M. Chi, J. Wang, S. Wang, S. Nie, Triboelectric probes for investigating charge transfer at the colloid-solid interface, Nano Energy 117 (2023), https://doi.org/10.1016/j.nanoen.2023.108874.

[26] S. Lin, C. Xu, L. Xu, Z.L. Wang, The overlapped Electron-Cloud model for electron transfer in contact electrification, Adv. Funct. Mater. 30 (2020), https://doi.org/10.1002/adfm.201909724.

[27] C. Xu, Y. Zi, A.C. Wang, H. Zou, Y. Dai, X. He, P. Wang, Y.-C. Wang, P. Feng, D. Li, Z.L. Wang, On the Electron-Transfer mechanism in the Contact-Electrification effect, Adv. Mater. 30 (2018) e1706790, https://doi.org/10.1002/adma.201706790.

[28] X. Huo, S. Li, B. Sun, Z.L. Wang, D. Wei, Recent progress of chemical reactions induced by contact electrification, Molecules 30 (2025), https://doi.org/10.3390/molecules30030584.

[29] Y. Zhao, Y. Liu, Y. Wang, S. Li, Y. Liu, Z.L. Wang, P. Jiang, The process of free radical generation in contact electrification at solid-liquid interface, Nano Energy 112 (2023), https://doi.org/10.1016/j.nanoen.2023.108464.

[30] H. Li, A. Berbille, X. Zhao, Z. Wang, W. Tang, Z.L. Wang, A contact-electro-catalytic cathode recycling method for spent lithium-ion batteries, Nat. Energy 8 (2023) 1137–1144, https://doi.org/10.1038/s41560-023-01348-y.

[31] W. Li, J. Sun, M. Wang, J. Xu, Y. Wang, L. Yang, R. Yan, H. He, S. Wang, W.-Q. Deng, Z.-Q. Tian, F.R. Fan, Contact-Electro-Catalysis for direct oxidation of methane under ambient conditions, Angew. Chem. (Int. Ed. Engl.) 63 (2024) e202403114, https://doi.org/10.1002/anie.202403114.

[32] J. Li, Y. Xia, X. Song, B. Chen, R.N. Zare, Continuous ammonia synthesis from water and nitrogen via contact electrification, Proc. Natl. Acad. Sci. USA 121 (2024) e2318408121, https://doi.org/10.1073/pnas.2318408121.

[33] S. Li, Z. Zhang, P. Peng, X. Li, Z.L. Wang, D. Wei, A Green approach to induce and steer chemical reactions using inert solid dielectrics, Nano Energy 122 (2024), https://doi.org/10.1016/j.nanoen.2024.109286.

[34] C. Xu, S. Li, Z. Yang, M. Willatzen, Z. Lin Wang, D. Wei, Contact-electro-luminescence triggered by triboelectric charge, Chem. Eng. J. 501 (2024), https://doi.org/10.1016/j.cej.2024.157754.

[35] D. Wei, T. Lindfors, C. Kvarnström, L. Kronberg, R. Sjöholm, A. Ivaska, Electrosynthesis and characterisation of poly(N-methylaniline) in organic solvents, J. Electroanal. Chem. 575 (2005) 19–26, https://doi.org/10.1016/j.jelechem.2004.08.018.

[36] J. Liu, Z. Yang, S. Li, Y. Du, Z. Zhang, J. Shao, M. Willatzen, Z.L. Wang, D. Wei, Nonaqueous Contact-Electro-Chemistry via triboelectric charge, J. Am. Chem. Soc. 146 (2024) 31574–31584, https://doi.org/10.1021/jacs.4c09318.

[37] Y. Su, A. Berbille, X.-F. Li, J. Zhang, M. PourhosseiniAsl, H. Li, Z. Liu, S. Li, J. Liu, L. Zhu, Z.L. Wang, Reduction of precious metal ions in aqueous solutions by contact-electro-catalysis, Nat. Commun. 15 (2024) 4196, https://doi.org/10.1038/s41467-024-48407-w.

[38] A. Berbille, X.-F. Li, Y. Su, S. Li, X. Zhao, L. Zhu, Z.L. Wang, Mechanism for generating H(2) O(2) at water-solid interface by contact-electrification, Adv. Mater. (Deerfield Beach Fla.) 35 (2023) e2304387, https://doi.org/10.1002/adma.202304387.

[39] Z. Wang, X. Dong, X.-F. Li, Y. Feng, S. Li, W. Tang, Z.L. Wang, A contact-electro-catalysis process for producing reactive oxygen species by ball milling of triboelectric materials, Nat. Commun. 15 (2024) 757, https://doi.org/10.1038/s41467-024-45041-4.

[40] Q.T. Trinh, N. Golio, Y. Cheng, H. Cha, K.U. Tai, L. Ouyang, J. Zhao, T.S. Tran, T.-K. Nguyen, J. Zhang, H. An, Z. Wei, F. Jerome, P.N. Amaniampong, N.-T. Nguyen, Sonochemistry and sonocatalysis: current progress, existing limitations, and future opportunities in Green and sustainable chemistry, Green. Chem. 27 (2025) 4926–4958, https://doi.org/10.1039/d5gc01098e.

[41] W. Lauterborn, T. Kurz, R. Geisler, D. Schanz, O. Lindau, Acoustic cavitation, bubble dynamics and sonoluminescence, Ultrason. Sonochem. 14 (2007) 484–491, https://doi.org/10.1016/j.ultsonch.2006.09.017.

[42] D.K. Bhui, H. Bar, P. Sarkar, G.P. Sahoo, S.P. De, A. Misra, Synthesis and UV–vis spectroscopic study of silver nanoparticles in aqueous SDS solution, J. Mol. Liq. 145 (2009) 33–37, https://doi.org/10.1016/j.molliq.2008.11.014.

[43] A. Henglein, Physicochemical properties of small metal particles in solution: "microelectrode" reactions, chemisorption, composite metal particles, and the atom-to-metal transition, J. Phys. Chem. 97 (2002) 5457–5471, https://doi.org/10.1021/j100123a004.

[44] S. Mondal, J.L. Montano-Priede, V.T. Nguyen, S. Park, J. Choi, V.H.M. Doan, T.M. T. Vo, T.H. Vo, N. Large, C.-S. Kim, J. Oh, Computational analysis of drug free silver triangular nanoprism theranostic probe plasmonic behavior for in-situ tumor imaging and photothermal therapy, J. Adv. Res. 41 (2022) 23–38, https://doi.org/10.1016/j.jare.2022.02.006.

[45] X. Sun, Y. Luo, Preparation and size control of silver nanoparticles by a thermal method, Mater. Lett. 59 (2005) 3847–3850, https://doi.org/10.1016/j.matlet.2005.07.021.

[46] F.Y. Alzoubi, A.A. Ahmad, I.A. Aljarrah, A.B. Migdadi, Q.M. Al-Bataineh, Localize surface plasmon resonance of silver nanoparticles using mie theory, J. Mater. Sci. Mater. Electron. 34 (2023), https://doi.org/10.1007/s10854-023-11304-x.

[47] Y. Nosaka, A.Y. Nosaka, Generation and detection of reactive oxygen species in photocatalysis, Chem. Rev. 117 (2017) 11302–11336, https://doi.org/10.1021/acs.chemrev.7b00161.

[48] Y. Nan, J. Shao, M. Willatzen, Z.L. Wang, Understanding contact electrification at Water/Polymer interface, Research 2022 (2022) 9861463, https://doi.org/10.34133/2022/9861463.
[49] D. Li, M. Xiong, S. Wang, X. Chen, S. Wang, Q. Zeng, Effects of low-temperature plasma treatment on wettability of glass surface: molecular dynamic simulation and experimental study, Appl. Surf. Sci. 503 (2020), https://doi.org/10.1016/j.apsusc.2019.144257.
[50] X.Q. Wang, W. Jian, O. Buyukozturk, C.K.Y. Leung, D. Lau, Degradation of epoxy/glass interface in hygrothermal environment: an atomistic investigation, Compos. Part B Eng. 206 (2021), https://doi.org/10.1016/j.compositesb.2020.108534.
[51] D. Dvoranova, Z. Barbierikova, V. Brezova, Radical intermediates in photoinduced reactions on TiO2 (an EPR spin trapping study), Molecules 19 (2014) 17279–17304, https://doi.org/10.3390/molecules191117279.
[52] Q. Yu, S. Ye, In situ study of oxygen reduction in dimethyl sulfoxide (DMSO) solution: a fundamental study for development of the Lithium–Oxygen battery, J. Phys. Chem. C. 119 (2015) 12236–12250, https://doi.org/10.1021/acs.jpcc.5b03370.
[53] R.H. Waghchaure, V.A. Adole, B.S. Jagdale, Photocatalytic degradation of methylene blue, rhodamine B, methyl Orange and eriochrome black t dyes by modified ZnO nanocatalysts: a concise review, Inorg. Chem. Commun. 143 (2022), https://doi.org/10.1016/j.inoche.2022.109764.
[54] P. Peerakiatkhajohn, T. Butburee, J.-H. Sul, S. Thaweesak, J.-H. Yun, Efficient and rapid photocatalytic degradation of methyl Orange dye using Al/ZnO nanoparticles, Nanomaterials 11 (2021), https://doi.org/10.3390/nano11041059.
[55] A.H. Haritha, M.E. Cruz, O. Sisman, A. Duran, D. Galusek, J.J. Velázquez, Y. Castro, Influence of annealing temperature on the photocatalytic efficiency of sol-gel dip-coated ZnO thin films in methyl Orange degradation, Open Ceram. 21 (2025), https://doi.org/10.1016/j.oceram.2024.100727.
[56] Q. Feng, Y. Tang, K. Wang, C. Wu, X. Huang, Study on the degradation of methyl Orange by UV-acetylacetone advanced oxidation system, Desalin. Water Treat. 321 (2025), https://doi.org/10.1016/j.dwt.2024.100928.
[57] N. Nagar, V. Devra, A kinetic study on the degradation and biodegradability of silver nanoparticles catalyzed methyl Orange and textile effluents, Heliyon 5 (2019) e01356, https://doi.org/10.1016/j.heliyon.2019.e01356.
[58] W. Zhang, T. Jiang, N. Li, S. Zhao, Y. Zhao, Enhanced photocatalytic degradation of methyl Orange by Metal-Tio2 nanoparticles, ChemistrySelect 9 (2024), https://doi.org/10.1002/slct.202401814.
[59] N. Gupta, H.P. Singh, R.K. Sharma, Metal nanoparticles with high catalytic activity in degradation of methyl Orange: an electron relay effect, J. Mol. Catal. A Chem. 335 (2011) 248–252, https://doi.org/10.1016/j.molcata.2010.12.001.
[60] V.K. Vidhu, D. Philip, Catalytic degradation of organic dyes using biosynthesized silver nanoparticles, Micron 56 (2014) 54–62, https://doi.org/10.1016/j.micron.2013.10.006.
[61] X. Zhao, Y. Su, A. Berbille, Z.L. Wang, W. Tang, Degradation of methyl Orange by dielectric films based on contact-electro-catalysis, Nanoscale 15 (2023) 6243–6251, https://doi.org/10.1039/d2nr06783h.
[62] A.M. Jones, S. Garg, D. He, A.N. Pham, T.D. Waite, Superoxide-mediated formation and charging of silver nanoparticles, Environ. Sci. Technol. 45 (2011) 1428–1434, https://doi.org/10.1021/es103757c.
[63] B. Chen, Y. Xia, R. He, H. Sang, W. Zhang, J. Li, L. Chen, P. Wang, S. Guo, Y. Yin, L. Hu, M. Song, Y. Liang, Y. Wang, G. Jiang, R.N. Zare, Water-solid contact electrification causes hydrogen peroxide production from hydroxyl radical recombination in sprayed microdroplets, Proc. Natl. Acad. Sci. USA 119 (2022) e2209056119, https://doi.org/10.1073/pnas.2209056119.
[64] C. Xia, S. Back, S. Ringe, K. Jiang, F. Chen, X. Sun, S. Siahrostami, K. Chan, H. Wang, Confined local oxygen gas promotes electrochemical water oxidation to hydrogen peroxide, Nat. Catal. 3 (2020) 125–134, https://doi.org/10.1038/s41929-019-0402-8.
[65] X. Shi, S. Back, T.M. Gill, S. Siahrostami, X. Zheng, Electrochemical synthesis of H2O2 by Two-Electron water oxidation reaction, Chem 7 (2021) 38–63, https://doi.org/10.1016/j.chempr.2020.09.013.
[66] J.G. Mahy, M. Kiendrebeogo, A. Farcy, P. Drogui, Enhanced decomposition of H2O2 using metallic silver nanoparticles under UV/Visible light for the removal of p-Nitrophenol from water, Catalysts 13 (2023), https://doi.org/10.3390/catal13050842.
[67] Y. Ono, T. Matsumura, N. Kitajima, S. Fukuzumi, Formation of superoxide ion during the decomposition of hydrogen peroxide on supported metals, J. Phys. Chem. 81 (2002) 1307–1311, https://doi.org/10.1021/j100528a018.
[68] D. He, A.M. Jones, S. Garg, A.N. Pham, T.D. Waite, Silver nanoparticle−reactive oxygen species interactions: application of a charging−discharging model, J. Phys. Chem. C. 115 (2011) 5461–5468, https://doi.org/10.1021/jp111275a.
[69] S. Lin, L. Xu, W.A. Chi, Z.L. Wang, Quantifying electron-transfer in liquid-solid contact electrification and the formation of electric double-layer, Nat. Commun. 11 (2020) 399, https://doi.org/10.1038/s41467-019-14278-9.
[70] C. Liu, A.J. Bard, Electrostatic electrochemistry at insulators, Nat. Mater. 7 (2008) 505–509, https://doi.org/10.1038/nmat2160.
[71] S. Lin, L.N.Y. Cao, Z. Tang, Z.L. Wang, Size-dependent charge transfer between water microdroplets, Proc. Natl. Acad. Sci. USA 120 (2023) e2307977120, https://doi.org/10.1073/pnas.2307977120.
[72] J. Zhang, M.L. Coote, S. Ciampi, Electrostatics and electrochemistry: mechanism and scope of Charge-Transfer reactions on the surface of tribocharged insulators, J. Am. Chem. Soc. 143 (2021) 3019–3032, https://doi.org/10.1021/jacs.0c11006.
[73] C.-y Liu, A.J. Bard, Electrostatic electrochemistry: nylon and polyethylene systems, Chem. Phys. Lett. 485 (2010) 231–234, https://doi.org/10.1016/j.cplett.2009.12.009.
[74] C.-y Liu, A.J. Bard, Chemical redox reactions induced by cryptoelectrons on a PMMA surface, J. Am. Chem. Soc. 131 (2009) 6397–6401, https://doi.org/10.1021/ja806785x.
[75] S. Li, J. Liu, Z.L. Wang, D. Wei, Mechano-driven chemical reactions, Green. Energy Environ. (2024), https://doi.org/10.1016/j.gee.2024.08.001.
[76] J.C. Barreto, G.S. Smith, N.H. Strobel, P.A. McQuillin, T.A. Miller, Terephthalic acid: a dosimeter for the detection of hydroxyl radicals in vitro, Life Sci. 56 (1995) PL89–PL96, https://doi.org/10.1016/0024-3205(94)00925-2.

Mohsin Shah received his M.S. degree in Physics from Central South University, where his research focused on micro- and nanoscale manipulation using electrostatic probes, combined with numerical analysis via finite element methods (FEM). He is currently pursuing his Ph.D. at the Beijing Institute of Nanoenergy and Nanosystems, Chinese Academy of Sciences, with his research primarily focused on contact electrification and its role in contact-electrochemistry (CE-chemistry).

Dr. Shaoxin Li is a post-doctor in the Beijing Institute of Nanoenergy and Nanosystems. She achieved the Ph.D degree from the University of Chinese Academy of Sciences in 2022 and the B.S. degree from the Jiangsu University in 2017. Her research interest is self-powered sensors, energy harvesting, and solid-liquid contact electrification.

Zhe Yang received his B.S. in Physics (2018) from Yantai University and M.S. in Physics (2022) from Shandong Normal University. Currently, he is a Ph.D. student at the Beijing Institute of Nanoenergy and Nanosystems, Chinese Academy of Sciences, with his research focuses on multiphase contact electrification mechanisms studied via density functional theory.

Jiajin Liu achieved his B. E. degree from the Jilin University in 2021. He is studying for a Ph.D. degree at the Beijing Institute of Nanoenergy and Nanosystems. His research interest is solid-liquid electrification and contact-electro chemistry.

Puguang Peng achieved the B.S. and M.S. degrees from the Xiangtan University in 2019 and 2022, respectively. He continues pursuing Ph.D. degree in Beijing Institute of Nanoenergy and Nanosystems, Chinese Academy of Sciences. His research mainly focuses on the ion dynamics modulation in nano-confined channels, which leads to high-performance iontronics energy and sensing applications, such as optical color recognition, wearable energy and e-textile.

Han Qian achieved the B.S. degree from Henan University of Science and Technology in 2023. He continues pursuing Ph.D. degree in Beijing Institute of Nanoenergy and Nanosystems, Chinese Academy of Sciences. He focuses on the transfer of ions and electrons at interfaces, with the applicatons in iontronics, osmotic energy conversion, and Contact-Electro-Chemistry **(CE-chemistry)**.

Prof. Zhong Lin Wang received his Ph.D. from Arizona State University in physics. He now is the Hightower Chair in Materials Science and Engineering, Regents' Professor, Engineering Distinguished Professor and Director, Center for Nanostructure Characterization, at Georgia Tech. Dr. Wang has made original and innovative contributions to the synthesis, discovery, characterization and understanding of fundamental physical properties of oxide nanobelts and nanowires, as well as applications of nanowires in energy sciences, electronics, optoelectronics and biological science. His discovery and breakthroughs in developing nanogenerators established the principle and technological road map for harvesting mechanical energy from environment and biological systems for powering personal electronics. His research on self-powered nanosystems has inspired the worldwide effort in academia and industry for studying energy for micro-nano-systems, which is now a distinct disciplinary in energy research and future sensor networks. He coined and pioneered the field of piezotronics and piezophototronics by introducing piezoelectric potential gated charge transport process in fabricating new electronic and optoelectronic devices. Details can be found at: http://www.nanoscience.gatech.edu.

Prof. Di Wei received his B.Sc. from the University of Science and Technology of China (USTC) and both his M.Sc. and Ph.D. from Åbo Akademi University in Finland. His research focuses on the applications of nanotechnology in energy and sensor systems. In this field, he has published over 120 papers in leading journals, including Nat. Energy, Nat. Commun., Sci. Adv., PNAS, Joule, Matter, Adv. Mater., Angew. Chem. Int. Ed., J. Am. Chem. Soc., Energ. Environ. Sci., Chem. Soc. Rev. etc. Wei holds a portfolio of over 200 international patents (including PCT filings), with nearly 100 successfully granted. Many of these patents have been transferred to leading companies such as Nokia in Finland and Lyten in the USA. Additionally, he has edited four English books published by Wiley and Cambridge University Press, among others. His contributions have been recognized with numerous accolades, including the First Prize of the Nokia Global Innovation and Excellence Award, the Brian Conway Prize in Physical Electrochemistry from the International Society of Electrochemistry (ISE), and various honors from ISE and the Royal Society of Chemistry (RSC). Details can be found at: http://www.iontronics.group/en/